Medicine in Novel Technology and Devices 11 (2021) 100075

Contents lists available at ScienceDirect

Medicine in Novel Technology and Devices

journal homepage: www.journals.elsevier.com/medicine-in-novel-technology-and-devices/

Full Length Article

A novel classification method for mild adolescent idiopathic scoliosis using 3D ultrasound imaging

D. Yang [a], T.T.Y. Lee [a], K.K.L. Lai [a], Y.S. Wong [b], L.N. Wong [a], J.L. Yang [d], T.P. Lam [b], R.M. Castelein [c], J.C.Y. Cheng [b], Y.P. Zheng [a,*]

[a] Department of Biomedical Engineering, The Hong Kong Polytechnic University, Hong Kong, China
[b] SH Ho Scoliosis Research Lab, Joint Scoliosis Research Center of the Chinese University of Hong Kong and Nanjing University, Department of Orthopaedics & Traumatology, The Chinese University of Hong Kong, Hong Kong, China
[c] Department of Orthopaedic Surgery, University Medical Center Utrecht, the Netherlands
[d] Spine Center, Xinhua Hospital Affiliated to Shanghai Jiaotong University School of Medicine, Shanghai, China

ARTICLE INFO

Keywords:
AIS classification
3D ultrasound
Mild AIS
Spine flexibility

ABSTRACT

Mild adolescent idiopathic scoliosis (AIS), with Cobb<20°, was hypothesized as the right stage to intervene to prevent progression. AIS curve can be categorized into either structural or non-structural depending on the spine morphology (flexibility). Using X-ray to characterize AIS curves remains the clinical gold standard while compromising the risks of radiation exposure. In previous works, 3D ultrasound imaging had proved the reliability of the coronal spinal curvature measurement. This research aimed at developing a mild AIS classification scheme through examining spine flexibility using 3D ultrasound imaging.

For the preliminary study, 90 mild AIS subjects (21 M and 69 F; Age:14.5 ± 1.7 years old; Cobb: 18.2 ± 6.4°) underwent both 3D ultrasound and X-ray scanning on the same day. For each case, a clinician measured Cobbs and denoted major curve as ground truth. Bending Asymmetry Index (BAI) was developed to indicate the presence of a possible structural curve. The curve classification was coded to a modified Lenke classification for mild cases (m-Lenke). The results of 3D ultrasound classification were evaluated with the X-ray.

It was shown that 70.1% of the subjects had identical curve classification results and 72.0% had the correct major curve detection. Lumbar-dominated curves had distinctive performance ($p = 0.91$, $r = 0.91$) against others. The study demonstrated the possibility of a 3D ultrasound-based method for mild AIS curve classification. The discrepancies could be partially explained by the limitations of the ultrasound scanning in proximal thoracic region. Subsequent studies will validate the proposed method with a larger cohort.

1. Introduction

Scoliosis, commonly defined as a lateral curvature of the spine. Over 70% are identified during or after puberty, known as adolescent idiopathic scoliosis (AIS) [1], with a prevalence of 0.47–5.2% [2]. Anatomically, AIS curve can be categorized into either structural (functional) or non-structural, depending on the skeletal morphology (spine flexibility), which requires distinct treatments [3,4]. Conventional non-surgical intervention methods, including exercise and bracing are adopted for non-structural curves [5,6] while surgery may be needed for severe structural ones [7]. It has been reported that AIS could deteriorate within months in the absence of proper intervention [8]. Classification schemes for AIS curves help formulate customized treatment strategies for individual patients. Most of the existing AIS classification schemes (Lenke, King, etc.) are for pre-surgery planning (Cobb > 40°) [9]. Categorization methods for mild AIS cases (Cobb < 25°) are yet to be raised. Mild AIS stage possesses significant curve progression risk: average 22%, and skyrockets to 68% once passing 20° [10]. Skalli's team identified deformation phenotypes for progression and suggested invention from mild curvatures [11]. Thus, the classification of mild AIS curve can be taken as an important preventive measure for follow-up scoliosis evaluation and treatments [12]. For mild AIS conditions, many exercise programs can be designed in clinical management, like pilates, scotch and other auto-correction practices [5,13]. It is of necessity that the possible structural sites of a mild AIS curve could be labelled, monitored and recorded; and customized measures could be applied to lessen or

* Corresponding author.
E-mail address: yongping.zheng@polyu.edu.hk (Y.P. Zheng).

https://doi.org/10.1016/j.medntd.2021.100075
Received 31 October 2020; Received in revised form 26 March 2021; Accepted 31 March 2021

alleviate the progression risk [14].

Using X-ray to characterize AIS curves remains the clinical gold standard, but with the risks of radiation exposure, thus cannot be used frequently [15,16]. In our previous works, Scolioscan (Telefield Medical Imaging Ltd, Hong Kong) had been demonstrated to be reliable for the coronal and sagittal spinal curvature measurement [17–19] through volume projection imaging (VPI) method [20–22]. This device has also been used for studying the spinal profile change during forward bending test [23] and measuring the spinal flexibility to assess the performance of the in-orthosis correction on AIS patients [24]. Apart from Scolioscan, several other free-hand 3D ultrasound systems have been reported for the assessment of spine deformity, and their main differences are the spatial sensors and ultrasound devices used, including optical sensing [25,26] and magnetic-field sensing transmitter [27–31]. They have been used for different applications, including flexibility test of spine [28]. Different scanning methods have been explored, including 2.5D extended view ultrasound imaging [32,33]. Recently studies have also been focused on more advanced processing for ultrasound images, including automatic curvature method using adaptive phase features in coronal images [34], vertebral surface detection [30]. Recently, Chen et al. (2020) demonstrated the feasibility of using a low-profile ultrasound scanner and magnet-field sensor to form a system [35]. All these studies have indicated that 3D ultrasound imaging can be a radiation-free candidate for X-ray complement in scoliosis assessment.

Therefore, the objective of this study is to evaluate whether a newly proposed 3D ultrasound-based AIS curve classification method could classify mild scoliotic curves accurately and effectively, which used the information provided by the coronal ultrasound images in standing and side bending postures. This work takes the pioneer role in categorization mild AIS curves with a radiation-free solution, which could be served as a post-screening analysis for clinician to assess the related treatment options in mild AIS management.

2. Materials and methods

2.1. Study design

This study retrospectively included 90 mild AIS subjects (21 M and 69 F; Age:14.5 ± 1.7 years old; Cobb: 18.2 ± 6.4°) from a schoolchildren screening program in Hong Kong. The female to male ratio was around 3:1, which was within the range mentioned in a previous study [1]. The subjects were clinically assessed in a single orthopedic spine unit from October 9, 2017 to September 24, 2018.

Bi-modality assessment was conducted using two systems, including low-dose X-ray EOS imaging system (EOS Imaging, France) and 3D ultrasound imaging system, Scolioscan (Model SCN801, Telefield Medical Imaging Ltd, Hong Kong). Each subject underwent both 3D ultrasound and X-ray scanning on the same day, including one standing X-ray with three ultrasound coronal images obtained under the postures of standing erect, left and right bending. To ensure the subjects could fully stretch their bodies to perform maximum bending on each side, an adjustable supporter was used to stabilize their postures during scanning.

2.2. Radiographic assessment

For classifying structural and non-structural scoliotic curves for mild AIS cases, a clinical group from Prince of Wales Hospital (Hong Kong) had extended the Scoliosis Research Society (SRS) standards for defining a scoliotic curve as a structural curve if both the upper and lower endplates of the curve have tilt angles > 5° (Upper Tilt Angle, UTA and Lower Tilt Angle, LTA) in practice [36]. Cobbs were measured for structural cases. The graphical illustration of the relationships of UTA, LTA and Cobb are shown in Fig. 1. Intuitively, when multiple curves were identified from the same subject, the largest Cobb measurement was marked as the major curve. The major curve would be given a high priority when evaluating the subsequent treatment options, as it had the largest impact on the spine morphology.

Patients were categorized using a modified version of the classical Lenke classification system for mild AIS (m-Lenke) using X-ray. The Lenke classification had been primarily adopted in scoliosis surgery planning, usually with a Cobb >40°. As our exploratory study attempted to classify mild curves, the numerical criteria were changed according to the above structural curve definition (Fig. 2). Similarly, the curve was characterized with its location of apex into either proximal thoracic (PT), main thoracic (T) or lumbar (L) curve.

For each case, a clinician measured Cobb angles and denoted the major curve from the standing X-ray radiographic as the ground truth. In case of no structural curve was found in a subject, the curve would be labelled as non-structural curve, and 'N/A' for major curve. Based on the location and magnitude of the structural curves from the same subject, the respective modified Lenke type and major curve could be obtained and used as a reference in comparison with the corresponding ultrasound results.

2.3. Ultrasound-based assessment and the 'BAI' calculation

Taking advantage of Scolioscan's radiation-free and flexible range of scanning [24], we proposed to locate the structural locations of AIS based on the fundamental biomechanics of spine. Nonstructural curves are commonly caused by muscle spasm, pain or certain disease and the curves can be restored in lateral bending; the structural curves are rigid and the spine is irreversibly altered in shape [4]. As shown in the illustration (Fig. 3), the curve maintaining its shape in lateral bending is marked as a structural curve; while the curve being corrected is a non-structural one. The dynamics of spine can be traced and reconstructed in three scanning postures: standing erect, left and right bending.

Each subject had taken whole-spine ultrasound scanning by Scolioscan from three postures: standing erect, bending to left and bending to right from posterior-anterior view (Fig. 4). In the proposed 3D ultrasound imaging processing method, a bending asymmetry index (BAI) was developed to indicate the presence of a possible location of structural sites through the discrepancy of a segment of spine from left/right bending (Fig. 5). Comparing the left/right bending ultrasound images, the discrepancies between two directional curves can be used to characterize the asymmetrical pattern of the spine: a large discrepancy may mean a rigid segment of spine which cannot be bent. In light of these conditions, we designed parameters that described such discrepancy to represent the possible structural curve location. With such principles, larger BAI could implicate a more severe structural curve. In addition, the curvature of the spine under the erect posture, i.e. erect spinous process angle (E-SPA), was measured automatically by a software developed in our research team previously [31]. If BAI paired with an E-SPA reading in the same level of the spine, the BAI value would be used to characterize the structural curve; otherwise, discarded. Similarly, the curve was characterized with its location of apex into either proximal thoracic (PT), main thoracic (T) or lumbar (L) curve. All these pieces of information could be codified into the table of modified Lenke classification system for mild AIS using 3D ultrasound in Fig. 2.

The block diagram shown in Fig. 6 illustrated the detailed process of generating BAI value, which includes the following step:

i. **Pre-processing:** annotate the center of all levels of spine (T1-L5) in the spinous line for three-posture ultrasound images and save all coordinates information; output the spinous process angle in erect stance (E-SPA) through the annotation software;
ii. **Image-processing:** interpolate spine curve with the coordinates from previous stage; flip and fuse lateral bending curves and derive the BAI through the calculation of the discrepancies of the curves;

iii. **Decision making:** generate the classification result based on the BAI and the related position in spine with conform to the modified Lenke classification table.

Figs. 7 and 8 demonstrated that how BAI could help identify non-structural and structural curves, respectively. As discussed, for non-structural curves, the curves are corrected during side bending; when mirroring the left/right bending curve, they are more or less matched with each other. For structural curves, the shapes of the curves persist during side bending. When mirroring the left/right bending curve, there would be discrepancies. Fig. 7 shows a case with a small curve in the ultrasound coronal image obtained under the erect standing posture, together with two bending curves (Fig. 7a). The extracted spine profiles under the bending postures are shown in Fig. 7b. As it can be observed in Fig. 7c, the two curves are almost identical, leading to a very small discrepancy when subtracting them. Therefore, the case shown in Fig. 7 is classified as nonstructural curve. Fig. 8 shows a typical case with structural curve. The procedure is the same as that described in Fig. 7, and the result shown in Fig. 8c indicates that there is an obvious discrepancy between the two curves, and the calculated BAI is 269.01 mm^2 (2330 $pixel^2$, 220ppi for ultrasound scanning), which implies a structural curve. The threshold of structural curve had been determined at 200 $pixel^2$ or 23.09 mm^2 empirically from a pilot run of the method with X-ray as reference among 33 subjects.

Similar as radiographic assessment, for each case, the measured BAI and denoted major curve (the largest BAI when multiple curves were presented) exacted from 3D ultrasound imaging analysis would be labelled and stored automatically. In case of no structural curve was found for a subject, the curve would be labelled as non-structural curve, and 'N/A' for major curve. Based on the location and magnitude of the structural curves from the same subject, the corresponding m-Lenke type and major curve could be obtained and used to compare with the X-ray findings.

3. Results

During the study period, 87 subjects were identified as eligible for inclusion. Three of them were excluded due to severe motion artifacts in the ultrasound imaging process.

Taking the classification results given by the EOS X-ray images as gold standard, out of the 87 patients, the number of m-Lenke type 1 to 6 is 8, 2, 10, 12, 23, and 5. In addition, there were two categories of curves could not be codified by the modified Lenke classification scheme: 1 patient had triple curves (similar to m-Lenke type 4), but the major curve was located in proximal thoracic region (denoted as PT*); 4 patients had structural curves in proximal thoracic and lumbar regions (denoted as PT + L), and nonstructural curve in main thoracic. Another 21 patients did not possess structural curves (denoted as NSC).

Referred to the X-ray classification results, the overall precision (p) of our proposed 3D ultrasound-based classification method was 0.70. The detailed m-Lenke classification results were presented in Fig. 9 and tabular form Table 1. From the results we could observe that the proposed method was feasible in characterizing lumbar or lumbar-dominated curve types (m-Lenke type 5 with $p = 0.91$, $r = 0.91$ & m-Lenke type 6 with $p = 0.80$, $r = 0.80$) and nonstructural scoliosis (NSC with $p = 1$, $r = 0.70$). For main thoracic-dominated and without the presence of proximal thoracic curve types (m-Lenke type 1 & 2 & 3), the proposed method also displayed certain effectiveness in classification. However, for the curve types that involved proximal thoracic curve (m-Lenke type 4 & variants), the performance of this classifier was challenged.

Similarly, the major curve identification results also adopted EOS X-ray films as gold standard. Of the 87 patients, 6 patients had proximal thoracic major curves (PT), 23 patients had main thoracic major curves (T), 37 patients had lumbar major curves (L), and 21 patients had no major curves as those were nonstructural (N/A). Compared with the X-ray results, the overall precision(p) of the proposed 3D ultrasound method for identifying major curve was 0.72. And the detailed statistics were available in Fig. 10 and Table 2. The results demonstrated similar trends as that in curve classification. The proposed method had distinctive power for lumbar-dominated curves ($p = 0.70$, $r = 0.90$) and non-structural ones ($p = 1$, $r = 0.70$). However, for the curve with main thoracic ($p = 0.52$, $r = 0.48$) or proximal thoracic curve ($p = 0.50$, $r = 1$) as major curve, the results were moderate.

4. Discussion

In this study, we reported that a new method based on 3D ultrasound imaging could provide an effective classification for mild AIS, particularly for the cases with lumbar-dominated curves (m-Lenke type 5 with $p = 0.91$, $r = 0.91$ & m-Lenke type 6 with $p = 0.80$, $r = 0.80$). According to a prevalence study of 72,699 schoolchildren, the most common type of mild AIS cases was thoracolumbar curves (40.1%) [38]. Our cohort of study also showed similar prevalence of lumbar/thoracolumbar curves (42.4%). It was quite constructive that our proposed method could accommodate the majority. From the promising results, the application of the proposed method could potentially reduce the use of X-ray in clinical management, tracking and evaluations for patients with lumbar curves. In addition, radiation-free follow-up programs could be specifically designed for the subjects with lumbar curves.

The method also demonstrated capability in classifying nonstructural curves ($p = 1$, $r = 0.70$). This finding was helpful in post-screening management of mild AIS subjects. Non-structural mild AIS cases usually required no follow-ups [a]. If these cases could be effectively removed from the lists of clinicians or therapists, the efficacies of the rehabilitation resources could be enhanced.

There were some limitations of the current method. If proximal thoracic curves were presented in the subject, no matter taking the dominant role or not, the curve classification results and major curve identification process may not live up to the expectation. The precision for m-Lenke type 4 classification was 0.08 (1 out of 12), and only 17.6% of the curves that contain proximal thoracic structural curves were correctly assorted. There were 7 failed cases in major curve detection: 3 cases had proximal thoracic as major curve and the other 4 had proximal thoracic as minor curve. This result was due to the physical limitation of the ultrasound scanning around proximal thoracic and cervical region, which has a convex surface and making the ultrasound coupling between the ultrasound probe and the skin be difficult, leading to poor image quality. A clinical study using 3D ultrasound imaging to investigate the measurement on thoracic spine also demonstrated that a lower reliability of measurement was found at upper thoracic segment compared with lumbar spine [39]. The development of a proper coupling method for ultrasound scanning for the upper thoracic and cervical region is needed, and flexible ultrasound arrays that could cover the whole spine region may be a good solution for the 'missing' curves in the proximal thoracic spine [40].

The method showed average classification results towards thoracic curves. The correctness of thoracic curves labelling was slightly over 50-50. Most of the failed cases were misclassifying into NSCs. After carefully reviewing these cases, it was found that the respective UTAs and LTAs were around 5°, which is the threshold value for determining structural or non-structural case. The decision-making process of the system was conducted without human's discretion, which could induce distinct classification decisions. In addition, in our previous research [31], we had demonstrated the linear relationship of ultrasound spinous process angle (SPA) with X-ray's Cobb. The thoracic-lumbar data combined correlation of SPA and Cobb was $y = 1.1797x$, $R^2 > 0.76$. This implies that angle measurements in 3D ultrasound images were slightly smaller than that in X-ray, which could also contribute to different decision made around the threshold value.

Another concern of the proposed method was raised for the cost-effectiveness of ultrasound scanning. As mentioned, the ultrasound-

derived parameter BAI required triple times of scanning: extra time and efforts were needed for the practice. Comparably, the benefits were outweighed the time consumption: it was first time to apply side bending ultrasound for curve classification. Clinicians could better manage the mild AIS subjects with timely and customized follow-ups.

The cohort of subjects of our study was obtained retrospectively from a government post-screening AIS program. The Lenke distribution of subjects was very uneven among different categories. In order to test the distinction power of the proposed method against specific type of AIS, a more even distribution of each class should be included in the further study when subject pool becomes statistically large; and we can understand the landscape of AIS classification better.

Last but not least, for this pilot study, one clinical expert was involved for the angle measurement and curve characteristics (start/end of the curve, curve apex) annotation. For our next step, we would like to investigate the intra- and inter-rater reliability of the proposed classification method for mild AIS with a large cohort.

5. Conclusion

This study proposed a new classification scheme for mild AIS based on 3D ultrasound imaging techniques together with bending tests, and its feasibility was successfully demonstrated. Because this new method is radiation-free, it can be widely used in any clinics serving non-surgical interventions for AIS, without the potential hazard of the traditional X-ray method. As demonstrated in this study, the new method was particularly suitable for classifying lumbar-dominated curves (m-Lenke type 4 & 5). Further studies should be conducted to test the validity and reliability of the proposed method to other categories of curves, as the cohort for this work had excessive number of lumbar curves. In addition, investigation could be made to seek a better coupling or new design of ultrasound probe in proximal thoracic region of spine.

Declaration of competing interest

The research has not yet been published, submitted or accepted for publication. This study was performed in line with the principles of the Declaration of Helsinki. Approval was granted by the Ethics Committee of the Hong Kong Polytechnic University (06 Sep 2018/ HSEARS20180906005).

Acknowledgements

This study is partially supported by Research Impact Fund of Hong Kong Research Grant Council(R5017-18) and Health and Medical Research Fund of the Hong Kong (04152896).

Appendix. Contents of Figures and Tables

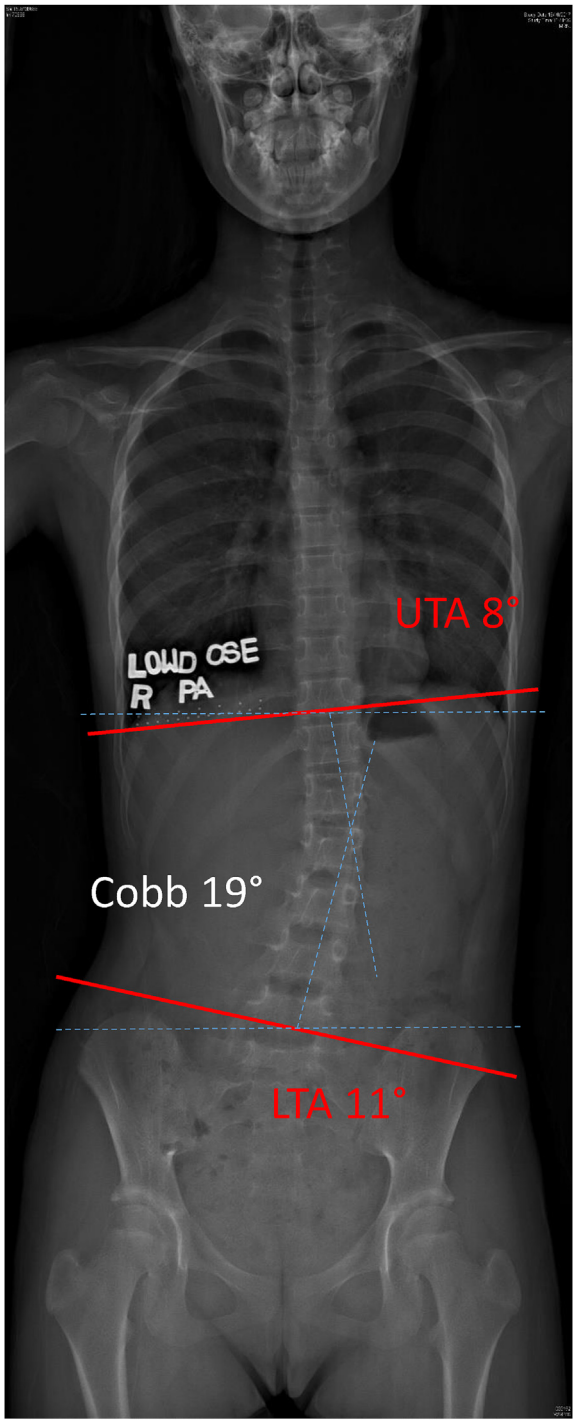

Fig. 1. Illustration of the concepts of Upper Tilt Angle (UTA), Lower Tilt Angle (LTA) and Cobb Angle.

The modified Lenke classification system for mild AIS				
Curve type	Proximal Thoracic	Main Thoracic	Thoracolumbar/ Lumbar	Description
1	Nonstructural	Structural*	Nonstructural	Main Thoracic
2	Structural	Structural*	Nonstructural	Double Thoracic
3	Nonstructural	Structural*	Structural	Double Major
4	Structural	Structural*	Structural*	Triple Major
5	Nonstructural	Nonstructural	Structural*	Thoracolumbar/Lumbar
6	Nonstructural	Structural	Structural*	Thoracolumbar/Lumbar – Main Thoracic

** Major curve, with largest Cobb measurement*

Location of apex	
Curve	Apex
Proximal Thoracic	T2-T5
Main Thoracic	T6-T12 Disk
Lumbar	T12-L4

	Structural criteria (X-ray)	Structural criteria (Ultrasound)
Proximal Thoracic	Upper Tilt Angle (UTA) of curve ≥ 5°; Lower Tilt Angle (LTA) of curve ≥ 5°	BAI value; SPA reading from erect ultrasound image
Main Thoracic	Upper Tilt Angle (UTA) of curve ≥ 5°; Lower Tilt Angle (LTA) of curve ≥ 5°	BAI value; SPA reading from erect ultrasound image
Thoracolumbar/Lumbar	Upper Tilt Angle (UTA) of curve ≥ 5°; Lower Tilt Angle (LTA) of curve ≥ 5°	BAI value; SPA reading from erect ultrasound image

Fig. 2. The details of the modified Lenke classification system for mild AIS (m-Lenke) (adapted from Ref. [9]), the structural criteria for X-ray and ultrasound are provided respectively.

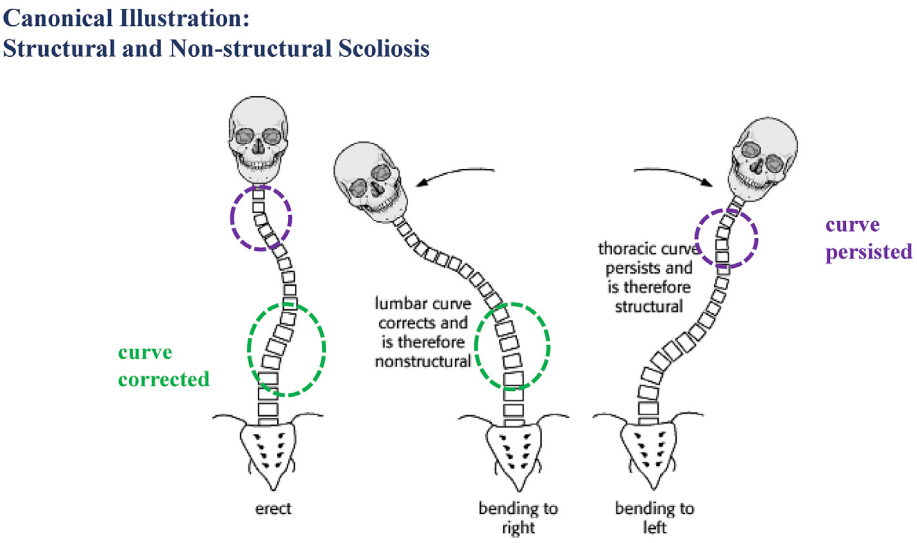

Fig. 3. Illustration of the fundamental biomechanics about different scoliosis curve types: structural curve (indicated by green circle) and non-structural curve (indicated by purple circle) [image courtesy: UW Radiology, [37].

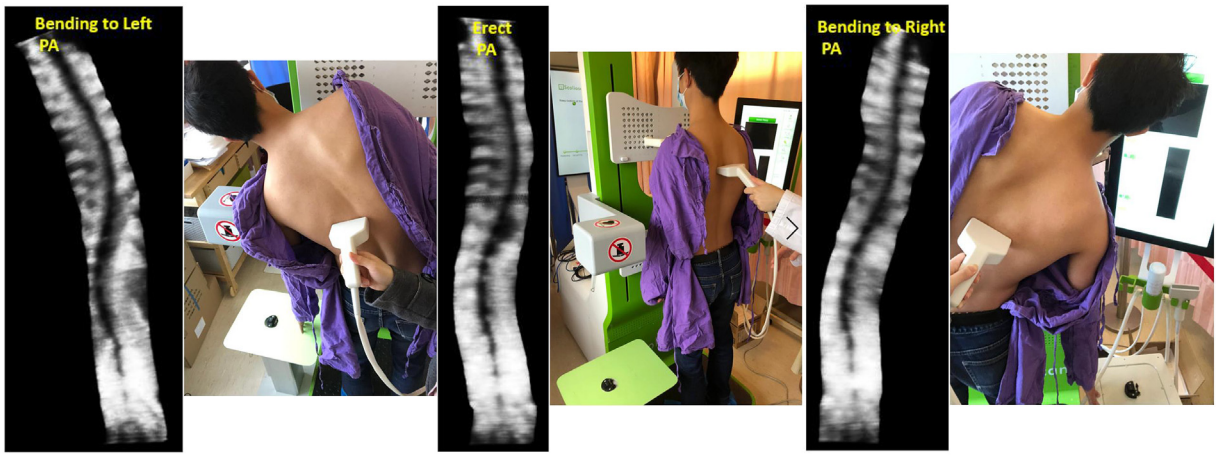

Fig. 4. Illustration of ultrasound scanning for three postures (from left to right): bending to left, standing erect and bending to right from posterior-anterior view.

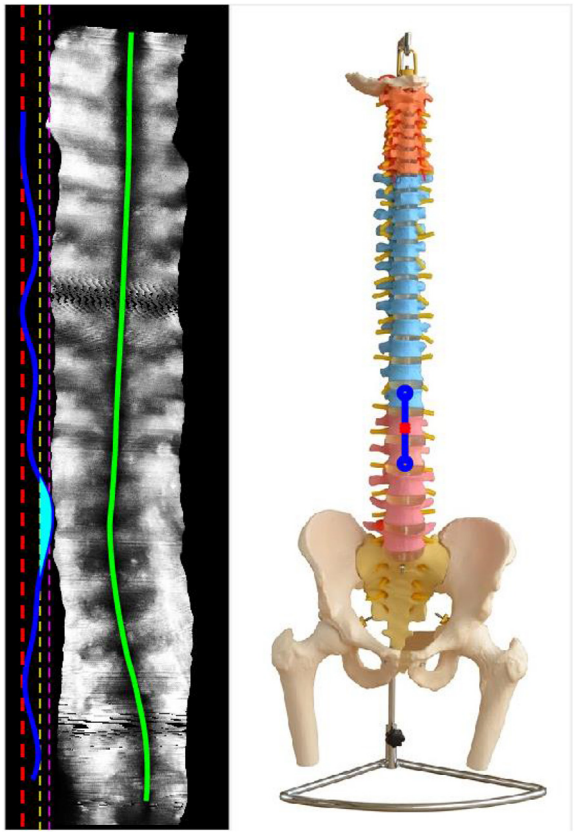

Fig. 5. Illustration of the representation of Bending Asymmetry Index (BAI). Line notation – blue line: bending discrepancy line (BDL); red line: pruned mean of the bending profile; purple line: absolute value of maximum of the bending profile; yellow line: standard error of mean of the bending profile; cyan area: bending asymmetry index (BAI).

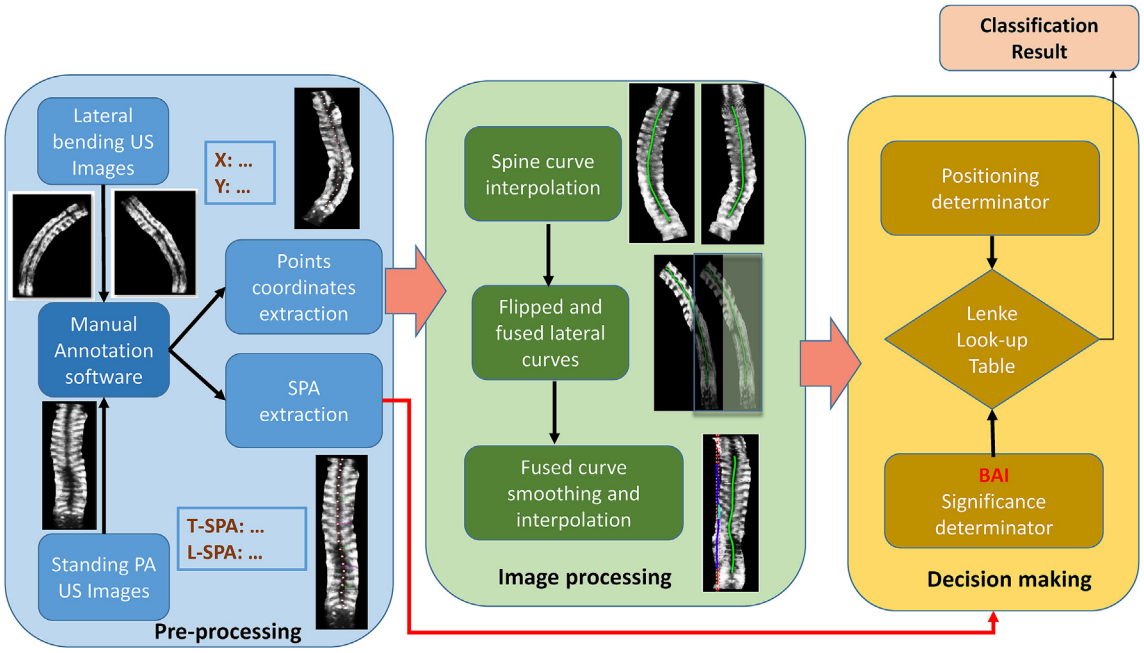

Fig. 6. Block diagram of the computer-aided BAI generation process. Pre-processing; Image processing and decision making.

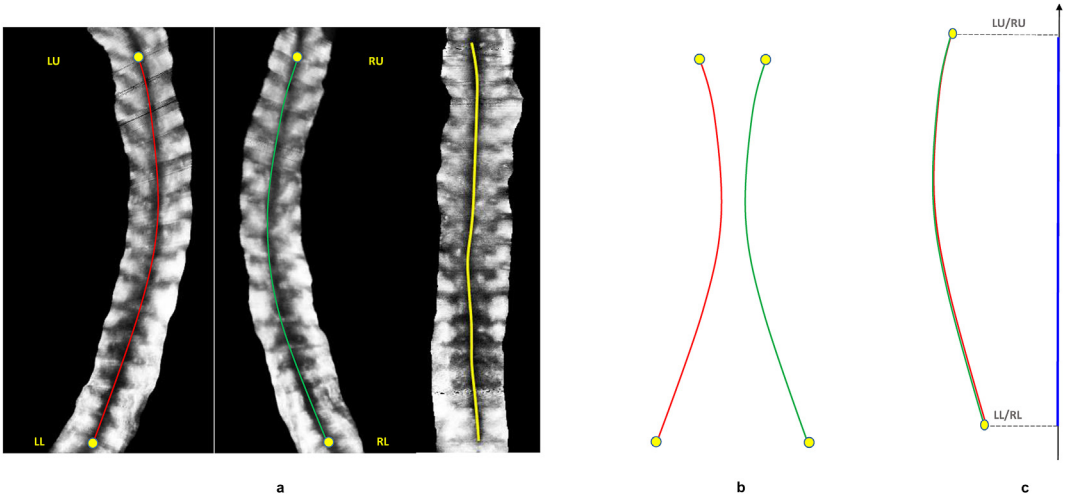

Fig. 7. Illustration of non-structural curve characterized by BAI from a typical subject. **(a)** An example of the three-posture coronal spine images from the same subject with the 3D ultrasound imaging method. The spinous lines (interpolated by the curve passing through centers of spinous process from all levels, T1-L5) for standing erect (E-SPL, yellow), bending to left (L-SPL, red) and bending to right (R-SPL, green) are super-imposed with the original ultrasound images with end points labelled with (Left/Right Upper/Lower) markers. **(b)** the extracted L-SPL and R-SPL from (a). **(c)** with alignment of end points, L-SPL is flipped to match with R-SPL to examine the asymmetrical pattern. For this curve, the BAI value is 90 pixel^2 or 10.39 mm^2, which is smaller than the threshold for structural curve (200 pixel^2 or 23.09 mm^2); it implicates that the thoraco-lumbar curve presented in E-SPL(a) is non-structural. Line notation (also applicable to Fig.8) – red line: line of the left bending spinous processes (L-SPA); green line: line of right bending spinous processes (R-SPA); yellow line: line of erect spinous processes (SPA); yellow circle: upper/lower points of line of spinous processes for alignment; blue line: bending discrepancy line (BDL); blue enclosed area: bending asymmetry index (BAI).

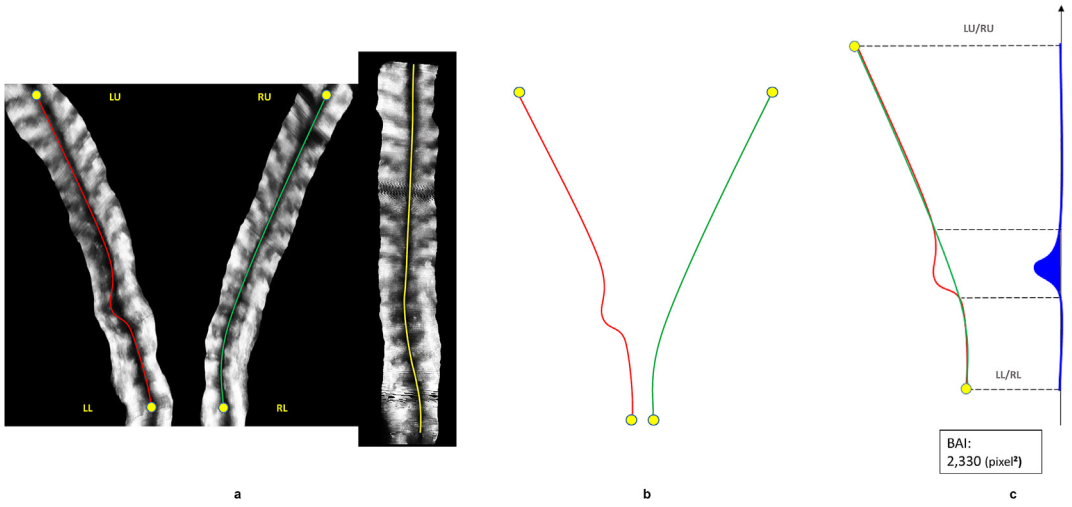

Fig. 8. Illustration of structural curve characterized by BAI from a real subject. **(a)** An example of three-posture coronal spine images from the same subject with the 3D ultrasound imaging method. The spinous lines (interpolated by the curve passing through centers of spinous process from all levels, T1-L5) for standing erect (E-SPL, yellow), bending to left (L-SPL, red) and bending to right (R-SPL, green) are super-imposed with the original ultrasound images with end points labelled with (Left/Right Upper/Lower) markers. **(b)** the extracted L-SPL and R-SPL from (a). **(c)** with alignment of end points, L-SPL is flipped to match with R-SPL to examine the asymmetrical pattern. For this curve, the BAI value is 2330 pixel^2 or 269.01 mm^2, which is larger than the threshold for structural curve (200 pixel^2 or 23.09 mm^2); it implicates that the thoraco-lumbar curve presented in E-SPL(a) is non-structural.

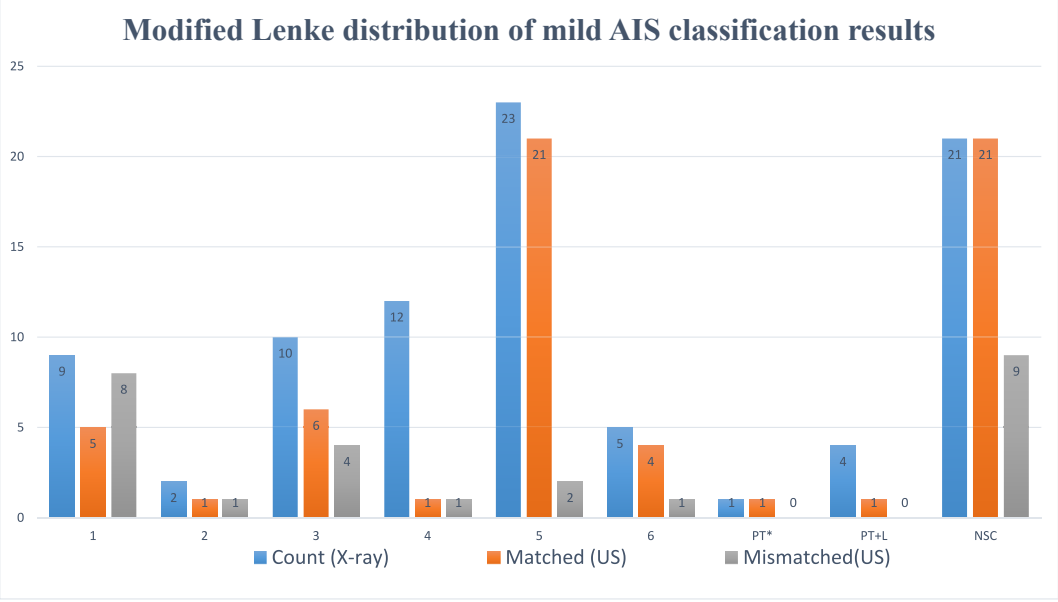

Fig. 9. The modified Lenke distribution of mild AIS classification (m-Lenke) results. Scolioscan 3D ultrasound classification results (Matched cases in orange, mismatched cases in grey) are compared with the gold-standard EOS X-ray classification results (blue). A matched case means both ultrasound and X-ray arrive at identical classification result. The ensemble comprises m-Lenke type 1–6 with two proximal thoracic-dominant variants: PT* (structural curve in proximal thoracic) and PT + L (structural curve in proximal thoracic and lumbar), and the detection of non-structural curves (NSC).

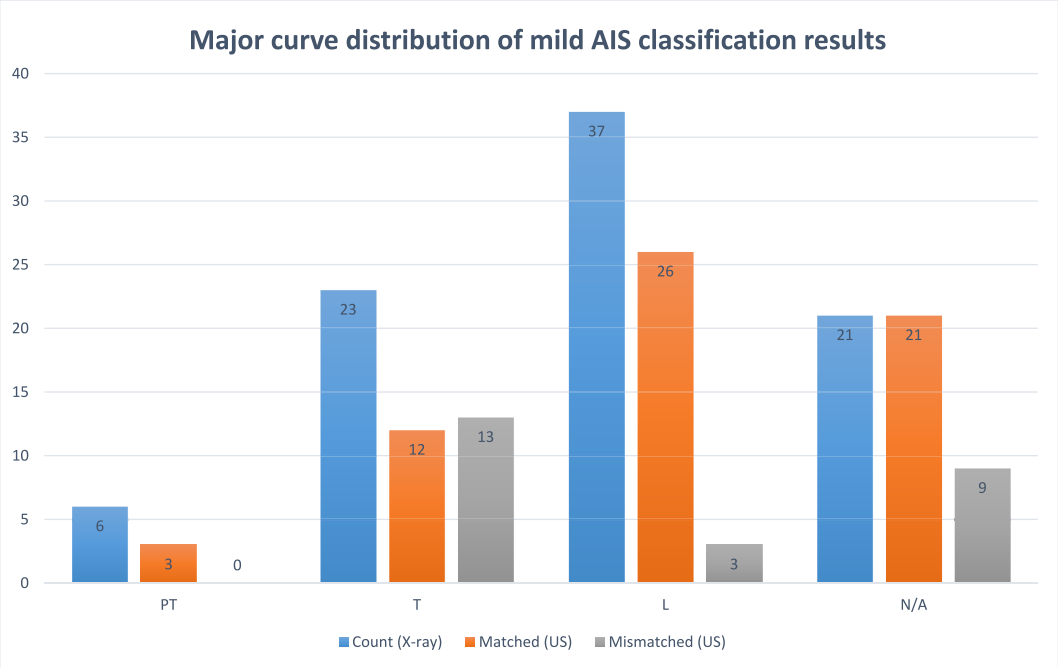

Fig. 10. The major curve distribution of mild AIS classification results. Scolioscan 3D ultrasound classification results (Matched cases in orange, mismatched cases in grey) are compared with the gold-standard EOS X-ray classification results (blue). A matched case means both ultrasound and X-ray arrive at identical major curve detection result. The ensemble comprises major curve located in proximal thoracic (PT), thoracic (T), lumbar (L) or not detected (N/A, for non-structural curves).

Table 1
Statistical analysis of the proposed AIS classification results

m-Lenke Type	Count (X-ray)Table 1	Matched (US)	Mismatched (US)	Precision (p)	Recall(r)
1	9	5	8	0.56	0.38
2	2	1	1	0.50	0.50
3	10	6	4	0.60	0.60
4	12	1	1	0.08	0.50
5	23	21	2	0.91	0.91
6	5	4	1	0.80	0.80
PT*	1	1	0	1	1
PT + L	4	1	0	0.25	1
NSC	21	21	9	1	0.70

Table 2
Statistical analysis of the major curve detection results

Major curve	Count (X-ray)	Matched (US)	Mismatched (US)	Precision (p)	Recall(r)
PT	6	3	0	0.50	1
T	23	12	13	0.52	0.48
L	37	26	3	0.70	0.90
N/A	21	21	9	1	070

References

[1] Weiss HR, Goodall D. The treatment of adolescent idiopathic scoliosis (AIS) according to present evidence. A systematic review. European Journal of Physical and Rehabilitation Medicine 2008;44(2):177–93. Jun 2008.

[2] Konieczny MR, Senyurt H, Krauspe R. Epidemiology of adolescent idiopathic scoliosis. J Child Orthop 2013;7:3–9. May 2013.

[3] Jada A, Mackel CE, Hwang SW, Samdani AF, Stephen JH, Bennett JT, Baaj AA. Evaluation and management of adolescent idiopathic scoliosis: a review. Neurosurg Focus 2017;43(4):E2. Oct 2017.

[4] Adams MA, Dolan P. Spine biomechanics. J Biomech 2005;38(10):1972–83. Oct 2005.

[5] Weinstein SL, Dolan LA, Cheng CY, Danielsson A, Morcuende JA. Adolescent idiopathic scoliosis. Lancet 2008;371(9623):1527–37. May 2008.

[6] Julien C, Carl-Eric A, Archana S, Hubert L, Stefan P. Correlation between immediate in-brace correction and biomechanical effectiveness of brace treatment in adolescent idiopathic scoliosis. Spine 2010;35(18):1706–13. Aug 2010.

[7] Rose PS, Lenke LG. Classification of operative adolescent idiopathic scoliosis: treatment guidelines. Orthop Clin N Am 2007;38(4):521–9. Oct 2007.

[8] Fong DYT, Cheung KMC, Wong YW, Wan YY, Lee CF, Lam TP, Cheng JCY, Ng BKW, Luk KDK. A population-based A population-based cohort study of 394,401 children followed for 10 years exhibits sustained effectiveness of scoliosis screening. Spine 2015;15(5):825–33. May 2015.

[9] Lenke LG, Edwards II CC, Bridwell KH. The Lenke classification of adolescent idiopathic scoliosis: how it organizes curve patterns as a template to perform selective fusions of the spine. Spine 2003;28(20S):S199–207. Oct 2003.

[10] Skalli W, Vergari C, Ebermeyer E, Courtois I, et al. Early detection of progressive adolescent idiopathic scoliosis, a severity index. Spine 2017;42(11):823–30. Jun 2017.

[11] Drevelle X, Lafon Y, Ebermeyer E, Courtois I, Dubousset J, Skalli W. Analysis of idiopathic scoliosis progression by using numerical simulation. Spine 2010;35(10):E407–12. May 2010.

[12] US Preventive Services Task Force. Screening for adolescent idiopathic scoliosis US preventive services task force recommendation statement. J Am Med Assoc 2018; 319(2):165–72. Jan 2018.
[13] Negrini S, Antonini G, Carabalona R, Minozzi S. Physical exercises as a treatment for adolescent idiopathic scoliosis. A systematic review. Journal of Pediatric Rehabilitation 2003;6(3):227–35. Sep 2003.
[14] Zapata KA, Sucato DJ, Jo CH. Physical therapy scoliosis-specific exercises may reduce curve progression in mild adolescent idiopathic scoliosis curves. Journal of Pediatric Physical Therapy 2019;31(3):280–5. Jul 2019.
[15] Altaf F, Gibson A, Dannawi Z, Noordeen H. Adolescent idiopathic scoliosis. Br Med J 2013;346:30–4. May 2013.
[16] Chamberlain CC, Huda W, Hojnowski LS, Perkins A, Scaramuzzino A. Radiation doses to patients undergoing scoliosis radiography. Br J Radiol 2000;73:847–53. May 2000.
[17] Cheung CWJ, Zhou GQ, Law SY, Lai KL, Jiang WW, Zheng YP. Freehand 3D ultrasound system for assessment of scoliosis. Journal of Orthopaedics Translation 2015;3(3):123–33. Jul 2015.
[18] Brink RC, Wijdicks SPJ, Tromp IN, Schlosser TPC, Kruyt MC, Beek FJA, Castelein RM. A reliability and validity study for different coronal angles using ultrasound imaging in adolescent idiopathic scoliosis. Spine 2017;18(6):979–85. Jun 2018.
[19] Lee TTY, Jiang WW, Cheng CLK, Lai KKL, To MKT, Castelein RM, Cheung JPY, Zheng YP. A novel method to measure sagittal curvature in spinal deformities: the reliability and feasibility of 3D ultrasound imaging. Ultrasound Med Biol 2019; 45(10):2725–35. Dec 2019.
[20] Cheung CW, Zhou GQ, Law SY, Mak TM, Lai KL, Zheng YP. Ultrasound volume projection imaging for assessment of scoliosis. IEEE Trans Med Imag 2015;34(8): 1760–8. Aug 2015.
[21] Zhou GQ, Jiang WW, Lai KL, Zheng YP. Automatic measurement of spine curvature on 3-D ultrasound volume projection image with phase features. IEEE Trans Med Imag 2017;36(6):1250–62. Jun 2017.
[22] Jiang WW, Zhou GQ, Lai KL, Hu SY, Gao QY, Wang XY, Zheng YP. A fast 3-D ultrasound projection imaging method for scoliosis assessment. Math Biosci Eng 2019;16:1067–81. May 2019.
[23] Jiang WW, Cheng CLK, Cheung JPY, Samartzis D, Lai KKL, Mkt T, Zheng YP. Patterns of coronal curve change in forward bending posture: a 3D ultrasound study of adolescent idiopathic scoliosis patients. Eur Spine J 2018;27(9):2139–47. May 2018.
[24] He C, To MKT, Cheung JPY, Cheung KMC, Chan CK, Jiang WW, Zhou GQ, Lai KKL, Zheng YP, Wong MS. An effective assessment method of spinal flexibility to predict the initial in-orthosis correction on the patients with adolescent idiopathic scoliosis (AIS). PloS One 2017;12(12). Dec 2017.
[25] Brignol A, Gueziri HE, Laporte C. Automatic extraction of vertebral landmarks from ultrasound images: a pilot study. Comput Biol Med 2020;122(May 2020):103838.
[26] Garbajal G, Gomez A, Ungi T, et al. Portable optically tracked ultrasound system for scoliosis measurement. Recent Advances in Computational Methods and Clinical Applications for Spine Imaging; 2015. 2015.
[27] Wang Q, Li M, Lou EHM, Chu WCW, Lam TP, Cheng JCY, Wong MS. Validity study of vertebral rotation measurement using 3D ultrasound in adolescent idiopathic scoliosis. Ultrasound Med Biol 2016;42(7):1473–81.
[28] Khodaei M, Zheng R, Lou EHM, et al. Intra-and inter-rater reliability of spinal flexibility measurements using ultrasound (US) images for non-surgical candidates with adolescent idiopathic scoliosis: a pilot study. Eur Spine J 2018;27:2156–64.
[29] Zheng R, Hill D, Lou EHM, et al. Assessment of curve progression on children with idiopathic scoliosis using ultrasound imaging method. Eur Spine J 2018;27:2114–9. 2018.
[30] Vo QN, Le LH, Lou EHM. A semi-automatic 3D ultrasound reconstruction method to assess the true severity of adolescent idiopathic scoliosis. Med Biol Eng Comput 2019;57:2115–28. 2019.
[31] Zheng YP, Lee TTY, Lai KKL, Yip BHK, Zhou GQ, Jiang WW, et al. A reliability and validity study for Scolioscan: a radiation-free scoliosis assessment system using 3D ultrasound imaging. Scoliosis and Spinal Disorders 2016;11(1):1. Sep 2016.
[32] Huang QH, Zeng ZZ, Li XL. 2.5-D extended field-of-view ultrasound. IEEE Trans Med Imag 2018;37(4):851–9. Apr 2018.
[33] Huang QH, Deng QF, Li L, et al. Scoliotic imaging with a novel double-sweep 2.5-dimensional extended field-of-view ultrasound. IEEE Trans Ultrason Ferroelectrics Freq Contr 2019;66(8):1304–15. Aug 2019.
[34] Zhou GQ, Li DS, Zhou P, Jiang WW, Zheng YP. Automating spine curvature measurement in volumetric ultrasound via adaptive phase features. Ultrasound Med Biol 2020;46(3):828–41. Oct 2020.
[35] Chen HB, Zheng R, Lou EHM, Le LH. Compact and wireless freehand 3D ultrasound real-time spine imaging system: a pilot study. Annu Int Conf IEEE Eng Med Biol Soc 2020:2105–8. Jul 2020.
[36] Korbel K, Kozinoga M, Stolinski L, Kotwicki T. Scoliosis research society (SRS) criteria and society of scoliosis orthopaedic and rehabilitation treatment (SOSRT) 2008 guidelines in non-operative treatment of idiopathic scoliosis. Polish Orthopedics and Traumatology 2014;79:118–22. May 2014.
[37] Department of Radiology, University of Washington. Scoliosis [Online] Available at: https://rad.washington.edu/about-us/academic-sections/musculoskeletal-radiology/teaching-materials/online-musculoskeletal-radiology-book/scoliosis/. [Accessed 16 December 2019].
[38] Wong HK, Hui JHP, Rajan U, Chia HP. Idiopathic scoliosis in Singapore schoolchildren: a prevalence study 15 years into the screening program. Spine 2005;30(10):1188–96. May 2005.
[39] Folsch C, Schlogel S, Lakemeier S, Wolf U, Timmesfeld N, Skwara A. Test-retest reliability of 3D ultrasound measurements of the thoracic spine. PMR 2012;4: 335–41. May 2012.
[40] Shea QTK, Yip PYM, Zheng YP. Development of flexible 2D ultrasound arrays for scoliosis assessment. In: IFMBE proceedings, Dec 2015; 2015. p. 256–8.